

# Achieving Domain Generalization in Underwater Object Detection by Image Stylization and Domain Mixup

Pinhao Song<sup>1,2</sup>, Linhui Dai<sup>1,2</sup>, Peipei Yuan<sup>1,2</sup>, Hong Liu<sup>1,2</sup> and Runwei Ding<sup>1,2</sup>

<sup>1</sup>Key Laboratory of Machine Perception, Shenzhen Graduate School, Peking University

<sup>2</sup>Peng Cheng Laboratory

{pinhaosong, dailinhui, peipeiyuan, hongliu}@pku.edu.cn, dingrunwei@pkusz.edu.cn

## Abstract

The performance of existing underwater object detection methods degrades seriously when facing domain shift problem caused by complicated underwater environments. Due to the limitation of the number of domains in the dataset, deep detectors easily just memorize a few seen domain, which leads to low generalization ability. Ulteriorly, it can be inferred that the detector trained on as many domains as possible is domain-invariant. Based on this viewpoint, we propose a domain generalization method from the aspect of data augmentation. First, the style transfer model transforms images from one source domain to another, enriching the domain diversity of the training data. Second, interpolating different domains on feature level, new domains can be sampled on the domain manifold. With our method, detectors will be robust to domain shift. Comprehensive experiments on S-UODAC2020 datasets demonstrate that the proposed method is able to learn domain-invariant representations, and outperforms other domain generalization methods. The source code is available at <https://github.com/mousecpn>.

## 1 Introduction

Object detection is a task that aims at identifying and localizing all objects of certain categories in an image. Object detection methods based on deep learning are also exploited in underwater robotic tasks, such as underwater robot picking, fish farming, biodiversity monitoring, and so on.

Compared with other conventional scenes, complicated underwater environments bring great challenges to underwater object detection since domain shift often happens in underwater environments. For example, different times in a day cause different light conditions, and water qualities vary greatly in different areas, such as lakes and oceans. Moreover, due to the enormous difficulties of collecting and annotating underwater images, it is hard to integrate a large underwater dataset with rich domain diversity. In practical use, it is unrealistic for detectors trained on the dataset with limited domain diversity to adapt to the changing underwater environments,

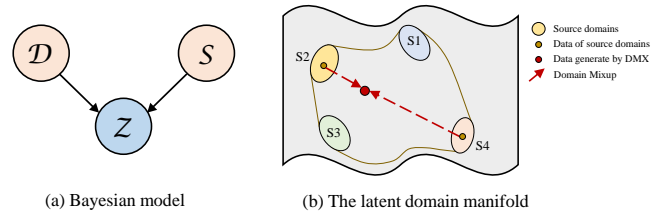


Figure 1: (a)  $\mathcal{Z}$  is the data distribution, which can be observed.  $\mathcal{D}$  is the domain distribution, and  $\mathcal{S}$  is the semantic contents distribution. (b) Each source domain occupies a very small area (the small ellipse in the Figure (b)), which can not represent the whole structure of the domain manifold. Domain Mixup can sample data inside the domain convex hull that is constructed by source domains.

resulting from detectors suffering from domain shift. Therefore, it is indispensable to drastically improve the detectors' robustness to domain shift.

The actual application in the wild can be seen as a domain generalization task that the model is trained on a series of source domains and evaluated on an unseen but related domain. Most of the previous works focus on aligning source domains, such as using MMD [Li *et al.*, 2018a] and adversarial training [Li *et al.*, 2018b]. Besides, current domain generalization works are devoted to recognition [Li *et al.*, 2017], but few works concern detection. Different from the works mentioned above, this paper proposes a domain generalization method for underwater object detection from the aspect of data augmentation. With a similar idea as [Somavarapu *et al.*, 2020; Xu *et al.*, 2019], our method increases the sampling on the domain distribution to improve the robustness to domain shift. As Figure 1 shows, the data distribution  $\mathcal{Z}$  depends on two prior distributions: the domain distribution  $\mathcal{D}$  and the semantic contents distribution  $\mathcal{S}$ .  $\mathcal{D}$  constructs a latent domain manifold. A small number of domains in the dataset can not represent the structure of the domain manifold, leading to domain overfitting. If more domains can be sampled for training, the detector will succeed in eliminating the effect of domain shift.

To this end, we propose an online data augmentation method to resolve the domain generalization problem of underwater object detection. First, the style transfer model named Bilateral Style Transfer (BST) is introduced to transform an underwater image from one source domain to an-

other. Second, Domain Mixup (DMX) on feature level is proposed to interpolate two different domains to synthesize a new one. Both of them increase the domain diversity of training data. Through training on the augmented features, the domain generalization capacity of the model can be improved by capturing the whole domain manifold.

In summary, the main contributions of this paper are summarized as follows:

- A style transfer model BST is leveraged to transform images from one source domain to another, enriching the domain diversity of the training data.
- A training paradigm named DMX is proposed to sample new domains on the domain manifold by interpolating paired images on feature level.
- Integrating two components mentioned above, a simple but effective data augmentation method is proposed to tackle the domain generalization problem for underwater object detection. Comprehensive experiments not only show that our method achieves superior performance on domain generalization tasks, but also prove the effectiveness of the proposed components.

## 2 Related Works

**Object Detection.** Existing object detection methods can be categorized into two groups, two-stage detectors and one-stage detectors. For two-stage detectors [Ren *et al.*, 2015; Wang *et al.*, 2017; Cai and Vasconcelos, 2018], the first stage is to use Region Proposal Network (RPN) to propose candidate object bounding boxes. In the second stage, detection head realizes classification and bounding boxes regression of all objects based on the features extracted by CNN and RoI Pooling. One-stage detectors [Liu *et al.*, 2016; Redmon and Farhadi, 2018] drop the use of RPN and RoI Pooling, directly regressing the coordinates of bounding boxes and classes of objects for real-time processing.

**Domain Adaptation and Generalization.** In domain adaptation problem, a source domain dataset with ground truth and an unlabeled target domain dataset are available. We hope to make full use of all these data during training and achieve good performance on target domain. In general, those two domains are related and share the same label space. A lot of works are proposed to solve domain adaptation in both recognition task and detection task, such as DANN [Ganin and Lempitsky, 2015], DA-FasterRCNN [Chen *et al.*, 2018], SW-FasterRCNN [Saito *et al.*, 2019], DM-ADA [Xu *et al.*, 2019], and DLOW [Gong *et al.*, 2019].

Domain generalization is a similar but harder task, in which the model is trained on a series of source domains and evaluated on an unseen but related domain. There are three kinds of ideas to achieve domain generalization. First, some works focus on aligning features of the source domains, such as CCSA [Motiian *et al.*, 2017], CIDDG [Li *et al.*, 2018b], and MMD-AAE [Li *et al.*, 2018a]. Second, data augmentation based methods aim to synthesize data to enrich domain diversity of training data, such as CrossGrad [Shankar *et al.*, 2018] and DGIS [Somavarapu *et al.*, 2020]. Third, self-supervised training is used to increase the robustness to

domain shift, such as JiGEN [Carlucci *et al.*, 2019]. However, a lot of domain generalization works stop at the recognition task, while domain generalization for object detection is understudied, which is what this paper focuses on.

**Real-time Style Transfer.** Early works on style transfer are optimization-based [Gatys *et al.*, 2016], which is extremely time-consuming. [Johnson *et al.*, 2016] proposes a real-time style transfer model with Conditional Instance Normalization (CIN), which can generate multiple styles without training multiple times, and achieves real-time processing. Besides, [Huang and Belongie, 2017] proposes an arbitrary real-time style transfer with Adaptive Instance Normalization (AdaIN). Recently, Bilateral Style Transfer (BST) [Xia *et al.*, 2020] proposes a photo-realistic arbitrary real-time style transfer based on the design of HDRNet [Li and Fang, 2019]. The style transfer models can be leveraged to achieve data augmentation.

## 3 The Proposed Method

The overview of our method is shown in Figure 2. Our method contains two components: BST and DMX. First, an image selected from one source domain is sent into BST to be converted to another source domain. Second, since paired images are obtained, DMX is applied on feature level during training, to sample new domains inside the domain convex hull constructed by source domains.

### 3.1 Bilateral Style Transfer (BST)

According to the Underwater Model mentioned in [Chiang and Chen, 2011], an underwater image  $I$  is linear transformed from the clear latent image  $J$  on color space. If two underwater images have the same clear latent image, they can be linear transformed from each other. Therefore, Bilateral Style Transfer [Xia *et al.*, 2020] is a reasonable choice to synthesize underwater images. Different from other style transfer models that directly generate output images, BST learns a local affine color transformation from a low-resolution style image and applies the transformation on the content image. First, a low resolution style image  $I_{s,low}$  is sent into the Coefficient Prediction Network  $F$ ,

$$A = F(I_{s,low}), \quad (1)$$

where  $A \in \mathbb{R}^{16 \times 16 \times 8 \times 3 \times 4}$  is the bilateral grid, and  $A[i, j, k] \in \mathbb{R}^{3 \times 4}$  is a affine color transformation matrix. Second, a content image  $I_c$  is fed into the Guidance Map Auxiliary Network  $P$  to obtain guidance map  $g$ ,

$$g = P(I_c), \quad (2)$$

where  $I_c \in \mathbb{R}^{H \times W \times 3}$ , and  $g \in \mathbb{R}^{H \times W \times 1}$ . Third, we upsample the bilateral grid using the guidance map,

$$\bar{A}[x, y] = \sum_{i,j,k} \tau(s_x x - i) \tau(s_y y - j) \tau(d \cdot g[x, y] - k) A[i, j, k] \quad (3)$$

where  $\bar{A}[x, y] \in \mathbb{R}^{3 \times 4}$ ,  $[x, y]$  is the pixel coordinates of the content image,  $s_x$  and  $s_y$  are the width and height ratios of the grid's dimensions w.r.t the full-resolution image's dimensions, and  $\tau(\cdot) = \max(1 - |\cdot|, 0)$ . Fourth, affine transform

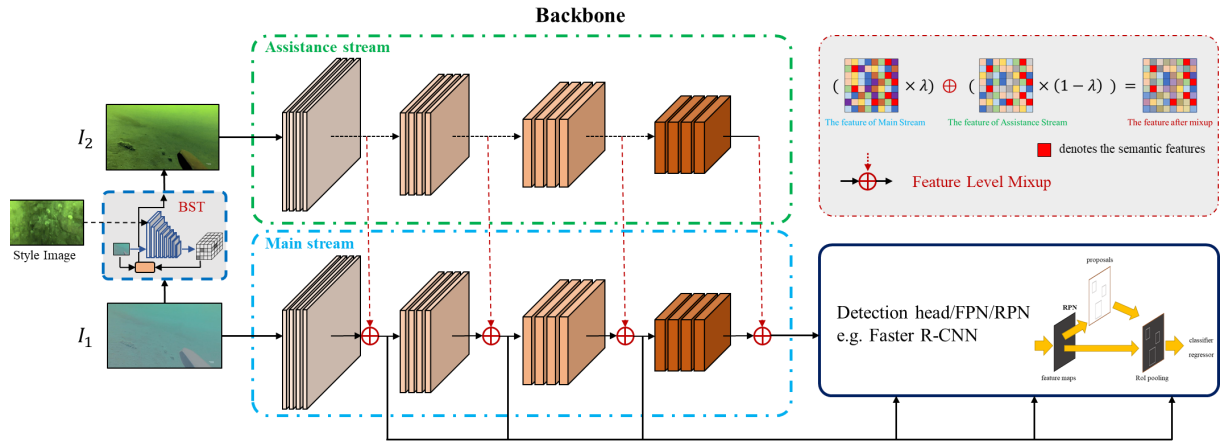


Figure 2: The overview of our proposed method. BST converts an image to another source domain. As the paired images of different domains with the same semantic contents are obtained, they are fed into the backbone simultaneously. Domain mixup is operated on the certain layers of the backbone. The red pixels in the feature maps denote the semantic features, while others are the irrelevant domain features.

is applied on the content image,

$$O[x, y] = I_c[x, y] \otimes \bar{A}[x, y][:, 0 : 3]^T + \bar{A}[:, 3]^T \quad (4)$$

$O \in \mathbb{R}^{H \times W \times 3}$  is the output image,  $O[x, y] \in \mathbb{R}^{1 \times 3}$ , and  $\otimes$  means matrix multiplication. Because most of the inference is performed at low resolution, BST achieves faster inference speed than other real-time style transfer models, which is suitable for online data augmentation.

### 3.2 Domain Mixup (DMX)

From BST, the original image  $I_1$  and its corresponding generated image  $I_2$  are obtained. In the backbone, the latent features of  $I_1$  and  $I_2$  contain two kinds of information: the domain information and the semantic information. Since the ground truth of  $I_1$  and  $I_2$  are the same, their latent semantic information is the same while the irrelevant domain information is different. If the latent features of  $I_1$  and  $I_2$  are interpolated, the semantic information is unchanged and the domain information is interpolated. Since the domain manifold is more flattened in the latent space than in the input space, linear interpolation can generate new domain inside the domain convex hull. Consider that  $K = [k_1, k_2, \dots, k_n]$  are the selected layers of the backbone to be performed mixup.  $I_1$  and  $I_2$  are fed into the backbone simultaneously (Main Stream and Assistance Stream). The features in Assistance Stream are used to augment the features of Main Stream. In Main Stream, the latent features can be expressed as:

$$h_{1,k} = \begin{cases} \lambda_k \cdot f_k(h_{1,k-1}) + (1 - \lambda_k) \cdot f_k(h_{2,k-1}), & k \in K \\ f_k(h_{1,k-1}), & \text{otherwise,} \end{cases} \quad (5)$$

while in Assistance Stream, the latent features can be expressed as:

$$h_{2,k} = f_k(h_{2,k-1}), \quad (6)$$

where  $k > 1$ ,  $f_k$  is  $k$ -th layer of the backbone,  $h_{1,k}$  and  $h_{2,k}$  is the feature maps of  $k$ -th layer of Main Stream and Assistance Stream respectively, and  $\lambda \sim \text{Beta}(\alpha, \alpha)$  is the mixup ratio of  $k$ -th layer, for  $\alpha \in (0, \infty)$ . We backpropagate gradient through both Main Stream and Assistance Stream. We

can use the features before Domain Mixup ( $f_k(h_{1,k-1})$  in  $k$ -th layer) or the features after Domain Mixup ( $h_{1,k}$  in  $k$ -th layer) in the Main Stream and feed them into the detection head. There are also two backpropagation way, which are backpropagating gradient through only Main Stream and through both of two streams. Using the features after Mixup for detection and backpropagating both streams is chosen in the experiments. All the variants mentioned above will be experimented in the ablation studies.

### 3.3 Discussion

We use  $\mathcal{Z}$  to represent the latent features of all layers. It can be assumed that the data distribution  $\mathcal{Z}$  has two independent prior distributions: the domain distribution  $\mathcal{D}$  and the semantic contents distribution  $\mathcal{S}$  (see Figure 1).  $\mathcal{D}$  constructs a latent domain manifold. From the perspective of Bayesian model, we can get:

$$\begin{aligned} p(\mathcal{S} | \mathcal{Z}) &= \int p(\mathcal{S}, \mathcal{D} | \mathcal{Z}) d\mathcal{D} \\ &= \int \frac{p(\mathcal{Z} | \mathcal{D}, \mathcal{S}) \cdot p(\mathcal{D}) \cdot p(\mathcal{S})}{p(\mathcal{Z})} d\mathcal{D} \quad (7) \\ &= E_{\mathcal{D}} \left[ \frac{p(\mathcal{Z} | \mathcal{D}, \mathcal{S}) \cdot p(\mathcal{S})}{p(\mathcal{Z})} \right]. \end{aligned}$$

The detector can be represented as  $q(\mathcal{S} | \mathcal{Z}, \theta)$  with learnable parameters  $\theta$ . The goal of the detector is to reduce the divergence between distribution  $p(\mathcal{S} | \mathcal{Z})$  and  $q(\mathcal{S} | \mathcal{Z}, \theta)$ . Leveraging Equation (4), the optimization goal is

$$\begin{aligned} & \text{argmin} \quad KL(p(\mathcal{S} | \mathcal{Z}) || q(\mathcal{S} | \mathcal{Z}, \theta)) \\ &= \text{argmin} \quad \int p(\mathcal{S} | \mathcal{Z}) \cdot \log \frac{p(\mathcal{S} | \mathcal{Z})}{q(\mathcal{S} | \mathcal{Z}, \theta)} d\mathcal{S} \quad (8) \\ &= \text{argmax} \quad E_{\mathcal{D}} [E_{\mathcal{S}} [p(\mathcal{Z} | \mathcal{D}, \mathcal{S}) \cdot \log q(\mathcal{S} | \mathcal{Z}, \theta)]] \end{aligned}$$

In the discrete condition, we can approximate  $p(\mathcal{Z} | \mathcal{D}, \mathcal{S})$  with empirical data distribution  $\frac{1}{N_{D,S}} \sum_{n=1}^{N_{D,S}} \delta_{Z_n}(\mathcal{Z})$  ( $N_{D,S}$

Detector	Method	Input size	Echinus(%)	Starfish(%)	Holothurian(%)	Scallop(%)	Ave.(%)
YOLOv3	DeepAll	416 × 416	70.28	31.83	27.67	41.74	42.88
	DANN (ICML'15)	416 × 416	63.67	24.01	25.78	30.28	37.32
	CrossGrad (ICLR'18)	416 × 416	71.21	31.41	32.17	32.46	41.81
	JiGEN (CVPR'19)	513 × 513	73.15	<b>38.56</b>	34.57	35.06	45.34
	DG-YOLO (ICIP'20)	416 × 416	62.74	26.83	32.84	34.54	39.24
	DGIS (ArXiv'20)	416 × 416	<b>74.59</b>	32.58	33.20	50.16	47.63
	<b>Ours</b>	416 × 416	73.26	36.69	<b>43.79</b>	<b>59.61</b>	<b>53.34</b>
Faster R-CNN	DeepAll	1333 × 800	74.79	36.59	43.12	40.94	48.86
	DANN (ICML'15)	1333 × 800	<b>78.62</b>	42.76	50.60	43.48	53.87
	CCSA (ICCV'17)	1333 × 800	76.71	36.85	40.58	37.46	47.90
	CrossGrad (ICLR'18)	1333 × 800	77.67	45.43	49.80	42.40	53.83
	MMD-AAE (CVPR'18)	1333 × 800	75.73	35.00	43.31	44.86	49.73
	CIDDG (ECCV'18)	1333 × 800	76.37	39.89	42.27	43.65	50.55
	JiGEN (CVPR'19)	768 × 768	76.15	39.06	50.27	41.44	51.73
	DGIS (ArXiv'20)	512 × 512	77.62	42.76	45.29	41.96	51.91
	<b>Ours</b>	512 × 512	77.06	<b>54.16</b>	<b>52.08</b>	<b>57.04</b>	<b>60.29</b>

Table 1: The performance of different domain generalization methods. Training dataset is source domains dataset of S-UODAC2020. "Ave." denotes the mAP@50 performance on target domain of S-UODAC2020, representing the domain generalization capacity of the model.

is the number of data with certain  $D$  and  $S$ ), and approximate the expectation in the optimization goal (8) by sampling on the domain distribution. The source domains of S-UODAC2020 are limited, occupying 6 small areas of the whole domain manifold. Without a large number of samples, the approximations are inaccurate. As a result, the model probably just "memorizes" these domains. A solution to this problem is to sample as many domains as possible for training. BST generates images of different domains with the same semantic contents, which can be seen as sampling on  $D$  given  $S$ . Assumed source domains construct a convex hull on the domain manifold, DMX can sample more domains inside the domain convex hull by interpolation.

## 4 Experiments

We will give an overview of how this section is organized. First, we introduce the dataset which experiments are implemented on. Second, our method is compared with other domain generalization methods and achieves better performance. Third, ablation studies and experiments on fewer source domains further prove its effectiveness. Fourth, to prove that BST is a better choice for our method, image quality, detection performance and inference speed comparisons are conducted with other real-time style transfer methods. Fifth, visualization of t-SNE [Maaten and Hinton, 2008] demonstrates that our method helps the model learn domain-invariant features.

### 4.1 Problem Statement and Dataset

Experiments are evaluated on Synthetic Underwater Object Detection Algorithm Contest 2020 (S-UODAC2020), which is generated from Underwater Object Detection Algorithm Contest 2020 (UODAC2020)<sup>1</sup>. UODAC2020 is randomly split into 7 sets on average, and each set contains 791 images. We transfer 7 sets to 7 domains (*type1* to *type7*) respectively

<sup>1</sup><http://uodac.pcl.ac.cn/>

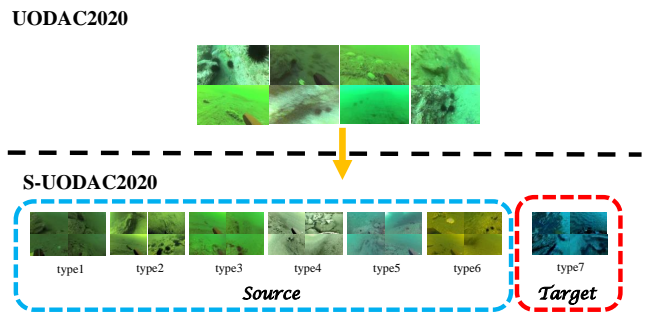


Figure 3: Illustration of S-UODAC2020 dataset.

by style transfer model  $WCT^2$  [Yoo *et al.*, 2019], in which *type1* to *type6* are source domains  $\mathcal{S}$  and *type7* is target domain  $\mathcal{T}$  (Figure 3). For source data  $x_s \in \mathcal{S}$ , class label  $c$  and bounding box coordinates  $b = [x, y, w, h]$  are available. Models should be trained on source domains and evaluated on target domain. Target domain data are totally not accessible during training.

### 4.2 Experiments in Domain Generalization Setting

**Experimental setup.** We apply our method on YOLOv3 and Faster R-CNN with FPN, which are widely used one-stage detector and two-stage detector respectively. Both models are trained on an Nvidia GTX 1080Ti GPU with PyTorch implementation. Models are trained on S-UODAC2020 training set (*type1-6*) and evaluated on S-UODAC2020 test set (*type7*). For YOLOv3, we train it for 100 epochs with batch size 8. Adam is employed for optimization with learning rate set to 0.001,  $\beta_1 = 0.9$ , and  $\beta_2 = 0.999$ . IoU, confidence, and NMS thresholds are set to 0.5, 0.02, 0.5 respectively. Accumulating gradient (every 2 iterations) are applied during training. We perform mixup on the features from layer 36, 46, 55, and 71 of DarkNet. Multi-scale training is used. For Faster R-CNN, we train it for 24 epochs with batch size 4. SGD

Method	Echinus(%)	Starfish(%)	Holothurian(%)	Scallop(%)	Ave.(%)
DeepAll	74.79	36.59	43.12	40.94	48.86
Only BST	76.88	49.09	50.49	56.23	58.17
BST+Input Mixup	75.56	47.72	46.43	47.19	54.23
BST+DMX*	76.79	51.96	51.26	57.20	59.30
Ouput Before Mixup	76.24	50.37	51.31	56.74	58.67
Detach Mixup	76.49	<b>55.10</b>	51.70	57.74	60.26
<b>Ours</b>	<b>77.06</b>	54.16	<b>52.08</b>	<b>57.85</b>	<b>60.29</b>

Table 2: Ablation study. "DMX\*" means mixup on feature level in a randomly chosen layer. "Output Before Mixup" means using the features before mixup for detection. "Detach Mixup" means backpropagating gradient through only Main Stream.

$\alpha$	0.1	0.5	1	2
mAP(%)	60.15	59.20	59.41	<b>60.29</b>

Table 3: Ablation study of the choice of  $\alpha$ . Mixup ratio  $\lambda \in \text{Beta}(\alpha, \alpha)$

Source	Method	mAP on type8
1-6	DeepAll	48.86
1-6	DANN	53.87
1-6	<b>Ours</b>	60.15
1-4	DeepAll	49.54
1-4	DANN	49.67
1-4	<b>Ours</b>	52.95
1-2	DeepAll	42.58
1-2	DANN	41.26
1-2	<b>Ours</b>	43.25

Table 4: The performance when it comes to fewer source domains. There are three groups of comparison, training on *type1-6*, *type1-4* and *type1-2*. All models are evaluated on *type7*.

is employed for optimization with learning rate, momentum and weight decay set to 0.02, 0.9 and 0.0001 respectively. IoU, confidence and NMS thresholds are set to 0.5, 0.05 and 0.5 respectively. We perform mixup on the features of every stage of ResNet-50. None of any other data augmentation methods except horizontal-flip is used unless we mention it.

#### Comparison with other domain generalization methods.

Since there are few domain generalization methods for object detection, we choose some of domain adaptation methods and domain generalization methods for recognition and modify them to fit for domain generalization of object detection. We compare the proposed method with the following methods. The implementation details of these methods can be seen in the supplementary materials.

- **DANN** [Ganin and Lempitsky, 2015] is a domain adaptation method, which uses a domain classifier to distinguish data from source and target for adversarial training. It is modified to distinguish data between source domains.
- **CCSA** [Motiian *et al.*, 2017] designs the Contrastive Semantic Alignment (CSA) loss to align the features of

Method	MST	AdaIN	BST
FPS	39.98	15.63	<b>78.62</b>
mAP	55.71	51.91	<b>58.17</b>

Table 5: Speed Comparison (in FPS) for  $512 \times 512$  images and performance comparison when being used for online data augmentation. Speeds are obtained with an Nvidia 1080Ti GPU and averaged over 100 images.

source domains.

- **CrossGrad** [Shankar *et al.*, 2018] follows the idea of defense of adversarial attack to augment the data.
- **MMD-AAE** [Li *et al.*, 2018a] aligns the features of source domains by adversarial learning and MMD loss.
- **CIDDG** [Li *et al.*, 2018b] uses class-conditioned and class prior-normalized domain classifier to perform domain adversarial training.
- **JiGEN** [Carlucci *et al.*, 2019] designs an auxiliary jigsaw puzzle task to increase the domain generalization capacity.
- **DG-YOLO** [Liu *et al.*, 2020] leverages adversarial training and IRM penalty to align features of source domains. It is re-trained and evaluated on S-UODAC2020 dataset.
- **DGIS** [Somavarapu *et al.*, 2020] is a data augmentation method by using image stylization to generate images across all source domains.

CCSA, MMD-AAE, and CIDDG are only implemented on Faster R-CNN in the R-CNN head, where detection task becomes instance classification. In Table 1, we can conclude that our method achieves much better performance than other methods in both YOLOv3 and Faster R-CNN. Also, it can be observed that domain generalization methods which are applied on image level (DANN, CrossGrad, JiGEN, and DGIS) are higher than those which work on instance level (CCSA, MMD-AAE, and CIDDG). It implies that the methods which perform well in the recognition task are not completely suitable for the detection task.

**Ablation study.** The results of the ablation study are shown in Table 2. If we choose source images and images generated by BST randomly for training ("Only BST"), the performance

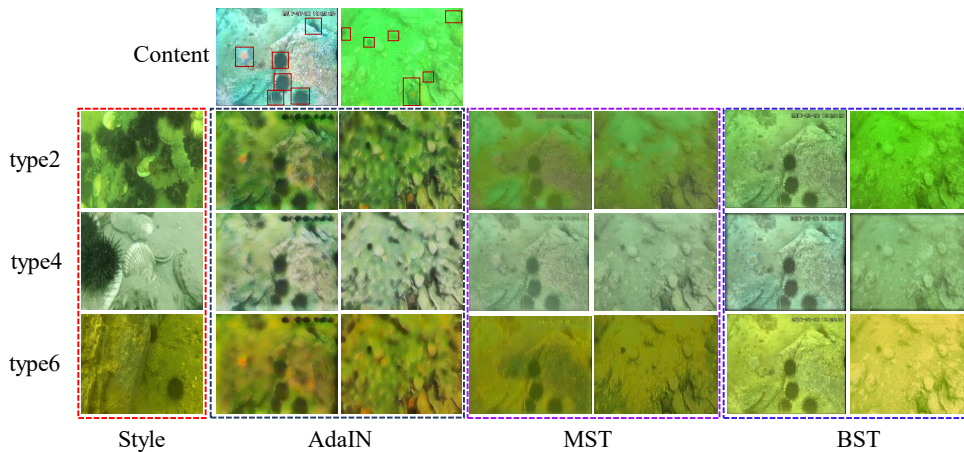


Figure 4: Qualitative comparison of our method against three state-of-the-art baselines on some challenging examples. We select three very different domains of S-UODAC2020 for the comparison.

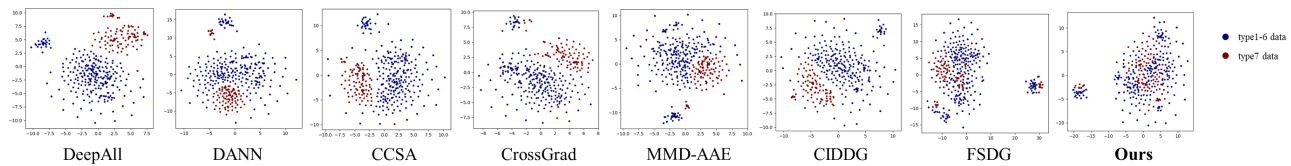


Figure 5: t-SNE visualization of different methods. Features are extracted from the last stage of ResNet with different methods. Blue points correspond to the source domains examples, while red points correspond to the target domain.

increases drastically compared with DeepAll. Mixup on input level [Zhang *et al.*, 2018] reduces the performance. This proves that the latent feature space is more flattened, so it is more reasonable to synthesize new domains by interpolation on feature level. And mixup on feature level in a randomly chosen layer [Verma *et al.*, 2019] can not achieve the same performance as our method. Using the features before mixup for detection (“Output Before Mixup”) has little increase on performance. If we backpropagate gradient through only Main Stream (“Detach Mixup”), the performance is almost equal to our method. Moreover, as shown in Table 3,  $\alpha = 2$  can achieve the best performance.

**Fewer source domains.** When the number of source domains decreases, does our method still perform well? Two more groups of experiments are set to find out the answer. From Table 4, our method outperforms DeepAll in all conditions. But the performance of DANN is lower than the performance of DeepAll in *type1-2* condition. This experiment further shows the effectiveness of our method when training on fewer source domains.

### 4.3 Experiments of Style Transfer Models

The experiment setting can be seen in the supplementary materials. The qualitative comparison is shown in Figure 4. The images AdaIN synthesizes are too stylized and not photo-realistic. MST blurs the objects which may limit the performance of detection. BST generates clear images with semantic contents well-protected. Besides, from Table 5, when we apply these style transfer models on the training of Faster R-CNN, BST obtains the highest performance, which is consis-

tent with qualitative comparison, and it also achieves fastest speed.

### 4.4 Visualization of t-SNE.

We use t-SNE projection to visualize the features distributions. We randomly select 300 images from source domains and 100 images from target domain, and input them into Faster R-CNN with different methods. The features of last stage of ResNet-50 is projected on the 2D plane (Figure 5). Blue points denote the data from source domains, while red points denote the data from target domain. If the red points are well merged with the blue points, the model captures more domain-invariant features. From the figures, it can be easily concluded that our method truly eliminates the effect of domain shift, while other methods somehow capture the spurious correlations.

## 5 Conclusion

In this paper, we focus on domain generalization for underwater object detection, which is an interesting but understudied problem. Our method leverages BST and DMX to enrich domain diversity of training data, increasing the sampling on the domain manifold. Trained with our method, the detector will be domain-invariant. In experiments, our method achieves better performance on S-UODAC2020 dataset compared with other domain generalization methods. Besides, further experiments prove the effectiveness and robustness of our method. We believe our method can promote the research of other domain adaptation and generalization task, such as autonomous

driving in the special weather (e.g. foggy or raining day), Re-ID in different light conditions (images of day and night), and so on.

## References

- [Cai and Vasconcelos, 2018] Zhaowei Cai and Nuno Vasconcelos. Cascade r-cnn: Delving into high quality object detection. In *CVPR*, pages 6154–6162, 2018.
- [Carlucci *et al.*, 2019] Fabio M Carlucci, Antonio D’Innocente, Silvia Bucci, Barbara Caputo, and Tatiana Tommasi. Domain generalization by solving jigsaw puzzles. In *CVPR*, pages 2229–2238, 2019.
- [Chen *et al.*, 2018] Yuhua Chen, Wen Li, Christos Sakaridis, Dengxin Dai, and Luc Van Gool. Domain adaptive faster r-cnn for object detection in the wild. In *CVPR*, 2018.
- [Chiang and Chen, 2011] John Y Chiang and Ying-Ching Chen. Underwater image enhancement by wavelength compensation and dehazing. *TIP*, 21(4):1756–1769, 2011.
- [Ganin and Lempitsky, 2015] Yaroslav Ganin and Victor Lempitsky. Unsupervised domain adaptation by backpropagation. In *ICML*, pages 1180–1189, 2015.
- [Gatys *et al.*, 2016] Leon A Gatys, Alexander S Ecker, and Matthias Bethge. Image style transfer using convolutional neural networks. In *CVPR*, pages 2414–2423, 2016.
- [Gong *et al.*, 2019] Rui Gong, Wen Li, Yuhua Chen, and Luc Van Gool. Dlow: Domain flow for adaptation and generalization. In *CVPR*, pages 2477–2486, 2019.
- [Huang and Belongie, 2017] Xun Huang and Serge Belongie. Arbitrary style transfer in real-time with adaptive instance normalization. In *ICCV*, pages 1501–1510, 2017.
- [Johnson *et al.*, 2016] Justin Johnson, Alexandre Alahi, and Fei-Fei Li. Perceptual losses for real-time style transfer and super-resolution. In *ECCV*, pages 694–711, 2016.
- [Li and Fang, 2019] Jinghui Li and Peiyu Fang. Hdrnet: Single-image-based hdr reconstruction using channel attention cnn. In *ICMSSP*, pages 119–124, 2019.
- [Li *et al.*, 2017] Da Li, Yongxin Yang, Yi-Zhe Song, and Timothy M Hospedales. Deeper, broader and artier domain generalization. In *ICCV*, pages 5542–5550, 2017.
- [Li *et al.*, 2018a] Haoliang Li, Sinno Jialin Pan, Shiqi Wang, and Alex C Kot. Domain generalization with adversarial feature learning. In *CVPR*, pages 5400–5409, 2018.
- [Li *et al.*, 2018b] Ya Li, Xinmei Tian, Mingming Gong, Yajing Liu, Tongliang Liu, Kun Zhang, and Dacheng Tao. Deep domain generalization via conditional invariant adversarial networks. In *ECCV*, pages 624–639, 2018.
- [Liu *et al.*, 2016] Wei Liu, Dragomir Anguelov, Dumitru Erhan, Christian Szegedy, Scott Reed, Cheng-Yang Fu, and Alexander C Berg. Ssd: Single shot multibox detector. In *ECCV*, pages 21–37, 2016.
- [Liu *et al.*, 2020] Hong Liu, Pinhao Song, and Runwei Ding. Towards domain generalization in underwater object detection. In *ICIP*, 2020.
- [Maaten and Hinton, 2008] Laurens van der Maaten and Geoffrey Hinton. Visualizing data using t-sne. *Journal of machine learning research*, 9(Nov):2579–2605, 2008.
- [Motiian *et al.*, 2017] Saeid Motiian, Marco Piccirilli, Donald A Adjeroh, and Gianfranco Doretto. Unified deep supervised domain adaptation and generalization. In *Proceedings of the IEEE International Conference on Computer Vision*, pages 5715–5725, 2017.
- [Redmon and Farhadi, 2018] Joseph Redmon and Ali Farhadi. Yolov3: An incremental improvement. *arXiv*, 2018.
- [Ren *et al.*, 2015] Shaoqing Ren, Kaiming He, Ross Girshick, and Jian Sun. Faster r-cnn: Towards real-time object detection with region proposal networks. In *NIPS*, pages 91–99, 2015.
- [Saito *et al.*, 2019] Kuniaki Saito, Yoshitaka Ushiku, Tatsuya Harada, and Kate Saenko. Strong-weak distribution alignment for adaptive object detection. In *CVPR*, pages 6956–6965, 2019.
- [Shankar *et al.*, 2018] Shiv Shankar, Vihari Piratla, Soumen Chakrabarti, Siddhartha Chaudhuri, Preethi Jyothi, and Sunita Sarawagi. Generalizing across domains via cross-gradient training. In *ICLR*, 2018.
- [Somavarapu *et al.*, 2020] Nathan Somavarapu, Chih-Yao Ma, and Zsolt Kira. Frustratingly simple domain generalization via image stylization. *arXiv preprint arXiv:2006.11207*, 2020.
- [Verma *et al.*, 2019] Vikas Verma, Alex Lamb, Christopher Beckham, Amir Najafi, Ioannis Mitliagkas, David Lopez-Paz, and Yoshua Bengio. Manifold mixup: Better representations by interpolating hidden states. In *ICML*, pages 6438–6447, 2019.
- [Wang *et al.*, 2017] Xiaolong Wang, Abhinav Shrivastava, and Abhinav Gupta. A-fast-rcnn: Hard positive generation via adversary for object detection. In *CVPR*, pages 2606–2615, 2017.
- [Wang *et al.*, 2019] Xudong Wang, Zhaowei Cai, Dashan Gao, and Nuno Vasconcelos. Towards universal object detection by domain attention. In *CVPR*, pages 7289–7298, 2019.
- [Xia *et al.*, 2020] Xide Xia, Meng Zhang, Tianfan Xue, Zheng Sun, Hui Fang, Brian Kulis, and Jiawen Chen. Joint bilateral learning for real-time universal photorealistic style transfer. *arXiv preprint arXiv:1409.7495*, 2020.
- [Xu *et al.*, 2019] Minghao Xu, Jian Zhang, Bingbing Ni, Teng Li, Chengjie Wang, Qi Tian, and Wenjun Zhang. Adversarial domain adaptation with domain mixup. In *AAAI*, 2019.
- [Yoo *et al.*, 2019] Jaejun Yoo, Youngjung Uh, Sanghyuk Chun, Byeongkyu Kang, and Jung-Woo Ha. Photorealistic style transfer via wavelet transforms. In *ICCV*, pages 7289–7298, 2019.
- [Zhang *et al.*, 2018] Hongyi Zhang, Moustapha Cisse, Yann N Dauphin, and David Lopez-Paz. mixup: Beyond empirical risk minimization. In *ICLR*, 2018.

## Supplementary

### Appendix A: Implementation details of other domain generalization method

- **DANN** [Ganin and Lempitsky, 2015] is a domain adaptation method, which uses a domain classifier to distinguish data from source and target for adversarial training. It is modified to distinguish data between source domains with a single domain classifier. In Faster R-CNN, the features of 2nd stage of ResNet are chosen for adversarial training, while in YOLOv3, the features of 36th layer of DarkNet are chosen.
- **CCSA** [Motiian *et al.*, 2017] designs the Contrastive Semantic Alignment (CSA) loss to align the features of source domains. The CSA loss is specially designed for recognition task (it uses

the class information), and it can be easily applied on the R-CNN head in Faster R-CNN for RPN and RoI Align decouple the classification and regression. But it is not suitable for YOLOv3. The negative proposals (background) do not participate in the CSA loss calculation.

- **CrossGrad** [Shankar *et al.*, 2018] follows the idea of defense of adversarial attack, and we just replace the loss of recognition with loss of detection. Domain classifier is set the same as DANN.
- **MMD-AAE** [Li *et al.*, 2018a] aligns the features of source domains by adversarial learning and MMD loss. It is only implemented on Faster R-CNN. The shared fc layer in the R-CNN head is regarded as the encoder with 1024 hidden neurons and the classification fc layer in the R-CNN head is the classifier. The decoder and discriminator with 2 fc layers is added to the R-CNN head.
- **CIDDG** [Li *et al.*, 2018b] uses class-conditioned and class prior-normalized domain classifier to perform domain adversarial training. It is only implemented on Faster R-CNN for the same reason as CCSA. All of the domain classifiers is applied on the features of the shared fc layer in the R-CNN head. The negative proposals do not participate in the adversarial training.
- **JiGEN** [Carlucci *et al.*, 2019] design an auxiliary jigsaw puzzle task to increase the domain generalization capacity. In Faster R-CNN, the features of last stage of ResNet are chosen for jigsaw puzzle task classification, while in YOLOv3, the features of 36th layer of DarkNet are chosen. Input sizes are  $513 \times 513$  and  $768 \times 768$  in YOLOv3 and Faster R-CNN respectively for breaking up the puzzle.
- **DG-YOLO** [Liu *et al.*, 2020] leverages adversarial training and IRM penalty to align features of source domains. It is re-trained and evaluated on S-UODAC2020 dataset.
- **DGIS** [Somavarapu *et al.*, 2020] is a data augmentation method by using image stylization to generate images across all source domains, which is similar to our method. DGIS uses AdaIN to perform image stylization. We implement "inter-domain" mode in the experiment.

## Appendix B: Experimental setup of style transfer model

We make comparison on three real-time style transfer models: AdaIN [Huang and Belongie, 2017], MST [Johnson *et al.*, 2016], and BST [Xia *et al.*, 2020]. Since BST has not been open-source yet, we reimplement it on the following training setting. BST is trained on an Nvidia GTX 1080Ti GPU with PyTorch implementation. We

randomly select images in S-UODAC2020 dataset as the style images. The training dataset used as content images is UODAC2020 training set. The trained model is validated on UODAC2020 validation set. The input size is  $512 \times 512$  both in training and inference. Adam is employed for optimization with learning rate set to 0.001,  $\beta_1 = 0.9$  and  $\beta_2 = 0.999$ . BST is trained for 10 epochs with batch size is 8. For MST, we randomly select one image from each source domain in S-UODAC2020 dataset as the style image, which means 6 fixed style images are used for training. Other training details are the same as BST. Since AdaIN is open-sourced, we can directly use its pre-trained model parameters.

## Appendix C: Experiment of mixup layer in ResNet-50

As is shown in Table 6, the experiment illustrates the effect of different mixup layer to the performance. The experiment is implemented on the Faster R-CNN with ResNet-50 as backbone. ResNet-50 contains 4 stages, and mixup can be perform on each stage. It can be observed that when we mixup all the stage of ResNet, we can obtain the highest performance. However, increasing the number of mixup layer can not guarantee performance improvement. From the third row to the fifth row, we can conclude that mixup on Medium depth leads to better performance compared with mixup shallowly and mixup deeply. Further, from the sixth row to the ninth row, mixup on the stage2 achieve better performance than other stage, which further proves that mixup on Medium depth has more benefit to domain generalization capacity. The reason is listed as follows: (1) in the shallow layer, the domain manifold is less flattened, so it is difficult for linear interpolation to generate new domains; (2) in the deep layer, most of the irrelevant domain information is discarded according to Information Bottleneck, so the diversity of sampled domains is decreased.

## Appendix D: Analysis of the features statistics.

A lot of works about style transfer [Huang and Belongie, 2017; Johnson *et al.*, 2016] show that there are some connections between normalization parameters ( $\gamma, \beta$ ) and styles, which can be interpreted that the features statistics of models are related to domains. Inspired by the analysis in [Wang *et al.*, 2019], we regard the features maps of each layer obey Gaussian distribution with certain mean and variance. In a domain-invariant model, the distribution of features from different domains will be closed to each other, which means they will have similar means and variances of different domains. We visualize the features statistics in Figure 6. 10 images are randomly selected from each domain, input into YOLOv3, and features are extracted from layer 12 to layer 58. In Figure 6(a-b), X-axis denotes layer indices, figures on the left denote mean of the features, and figures on the right denote variance of the features.

Stage1	Stage2	Stage3	Stage4	Echinus(%)	Starfish(%)	Holothurian(%)	Scallop(%)	Ave.(%)
✓	✓	✓	✓	77.06	54.16	52.08	57.85	<b>60.29</b>
✓	✓	✓		77.38	50.45	<b>52.82</b>	54.76	58.85
		✓		<b>77.69</b>	<b>55.49</b>	50.37	57.26	60.20
			✓	76.20	52.53	51.41	58.59	59.68
✓				76.66	52.62	51.59	<b>58.73</b>	59.90
	✓			76.74	54.50	49.03	57.40	59.42
		✓		76.17	52.57	50.74	56.60	59.02
			✓	76.52	54.75	51.18	57.04	59.87

Table 6: Ablation study of mixup stage.



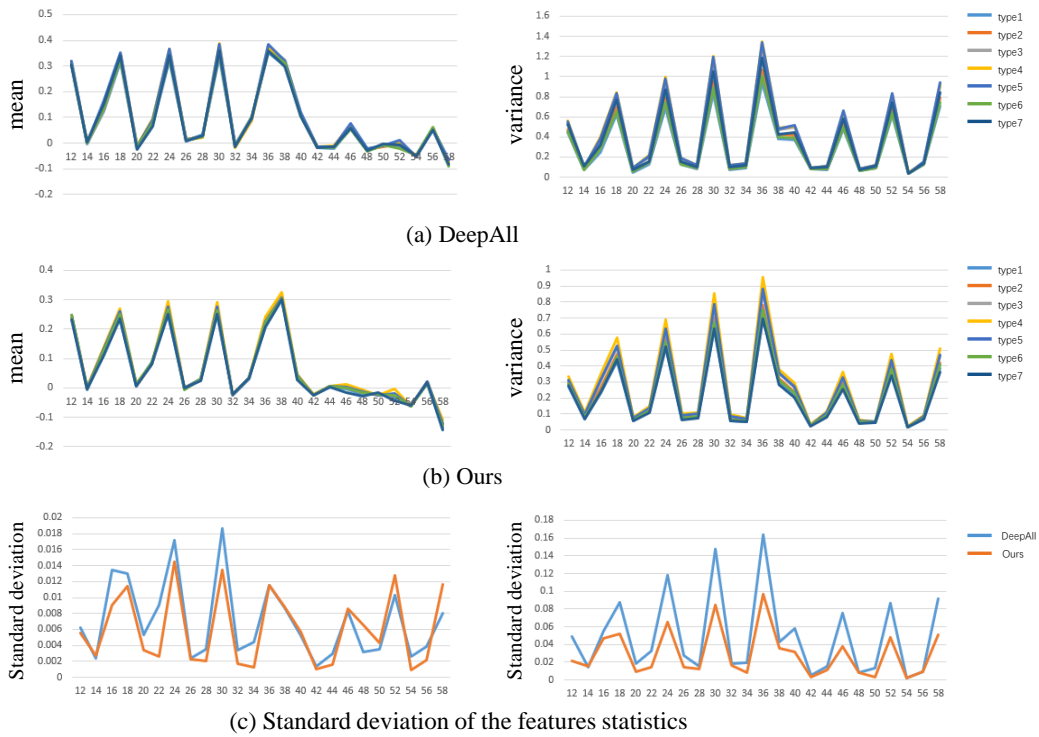


Figure 6: Visualization of the features statistics.

For (a), the model trained on source domains is analyzed. Each line in (a) represents the mean (left) or the variance (right) of the features from the 10 images in a certain layer. For (b), the model trained with our method is analyzed. For (c), we calculate the standard deviation of the mean (left) and variance (right) of *type1-7* for each layer. High standard deviation means that the features distributions of different domains are very different and the model suffers from domain shift, while small standard deviation denotes the strong robustness to domain shift. From 6(c), the standard deviation of features statistics of our methods is smaller than DeepAll in most of the layers. This visualization shows that our method helps model learn the domain-invariant features.